Indian Journal of Chemical Technology
Vol. 25, September 2018, pp. 475-481

Green synthesis of silver nanoparticles using *Coccinia grandis* fruit extract and its application toward the reduction of toxic nitro compounds

Th. Babita Devi & M Ahmaruzzaman*
National Institute of Technology Silchar 788 010, Assam, India
E-mail: mda2002@gmail.com

Received 16 September 2016 ; accepted 24 July 2017

Silver nanoparticles have been synthesized using *Coccinia grandis* fruit extract without using any surfactant or external energy. The phytochemical present in the fruit acts as a reducing agent and reduced the metal ions (Ag^{+}) into metallic form (Ag^{0}) and help in the formation of silver nanoparticles. For further confirmation, synthesized silver nanoparticles are well characterized by using UV-Visible spectroscopy, TEM, XRD, FT-IR and EDX techniques. The catalytic activities of nanoparticles in the reduction of toxic nitro compounds such as para nitrophenol and para nitroaniline has also been investigated. It is observed that silver nanoparticles show excellent catalytic activity towards the reduction of toxic nitro compounds. This is for the first time, the synthesis of silver nanoparticle using *Coccinia grandis* fruit extract has been reported.

Keywords: Biosynthesis, Nanoparticles, Plants, Reduction, Silver.

Metal nanomaterials have received tremendous scientific and practical interest due to their unique properties and novel applications compared to their bulk counterparts[1–5]. A variety of chemical and physical procedures have been used for synthesis of metallic nanoparticles. However, these methods are accompanied by many problems including use of toxic solvents, generation of hazardous by-products, costly machine, longer time and high energy consumption. Accordingly, there is an essential need to develop environmentally benign procedures for synthesis of metallic nanoparticles. A promising approach to achieve this objective is to exploit the array of biological resources in nature. Many researchers has been reported to till date on biological syntheses of metallic nanoparticles using microorganisms including bacteria[6], fungi[7] and plants[8-10] because of their antioxidant or reducing properties typically responsible for the reduction of metal compounds in their respective nanoparticles. Although among the various biological methods of metallic nanoparticles synthesis, microbe mediated synthesis is not of industrial feasibility due to the requirements of highly aseptic conditions and their maintenance.

To overcome this drawback plant extracts were used for the synthesis of nanoparticles. These green routes eliminate the use of expensive chemicals and are eco-friendly. Phytochemical compounds such as saponins, phenolic compounds, phytosterols and quinines present in plant biomolecules have both preservative and reductive activity. Keeping in view shortcoming of the previous studies, we design a novel and totally green method for the synthesis of Ag nanoparticles using *Coccinia grandis* fruit extract. A large number of plants are already reported to facilitate silver nanoparticles synthesis and some of them are mentioned in this article in Table 1[8-21]. Synthesis of metallic nanoparticles is done by using different parts of plant such as stem, root, leaves, flower and seed (Table 1). The literature review reveals that no synthesis method has been reported for preparation of Ag nanoparticles using *Coccinia grandis* fruit extract. In the present work, Ag nanoparticles were synthesized without using any reducing and stabilizing agent. The phyto-chemical present in the fruit extract is acted as a reducing agent in the formation of NPs[20-22]**.** The prepared nanoparticles are well characterized by XRD, TEM, HR-TEM, SAED, FT-IR, SEM-EDX and UV-visible spectroscopy.

We have also investigated the catalytic properties of the synthesized silver nanoparticles. The synthesized Ag nanoparticles are showed an excellent catalytic property in the reduction of *para* nitrophenol and *para* nitroaniline in aqueous medium. Approximately 98.3%, 98.1% of *para* nitrophenol and *para* nitroaniline are reduced using Ag nanoparticles (catalyst).

Experimental Section

Material

The starting materials were of AR grade Silver nitrate ($AgNO_3$), *para* nitrophenol (PNP), *para* nitroaniline (PNA) and sodium borohydride ($NaBH_4$) obtained from Merck India Limited Chemicals and used without any further purification. All solutions were prepared in double-distilled water and all

Table 1— Green synthesis of silver nanoparticles by different researchers using plant extracts

Plants	Plants size(nm)	Plants part	Shape	Reference
Acorous calamus	31.83	Rhizome	Spherical	[8]
Tea extract	20–90	Leaves	Spherical	[9]
Sesuvium portulacastrum L	5-20	Leaves	Spherical	[10]
Cocous nucifera	22	Inflorescence	Spherical	[11]
Pistacia atlantica	10–50	Seeds	Spherical	[12]
Ziziphora tenuior	8-40	Plant	Spherical	[13]
Nelumbo nucifera	25–80	Leaves	Spherical, triangular	[14]
Acalypha indica	20–30	Leaves	Spherical	[15]
Premna herbacea	10–30	Leaves	Spherical	[16]
Boerhaavia diffusa	25	Whole plant	Spherical	[17]
Tribulus terrestris	16–28	Fruit	Spherical	[18]
Abutilon indicum	7–17	Leaves	Spherical	[19]
Coccinia grandis	20-30	Leaves	Spherical	[20]
Coccinia grandis	100	Flower	---	[21]
Coccinia grandis	10-15	Fruit	Spherical	Present work

apparatus were rinsed with aqua regia (3:1 solution of HCl: HNO_3) and then washed with double-distilled water before use.

Preparation of *Coccinia grandis* fruit extract

Locally available fresh fruit of *Coccinia grandis* was taken from Silchar Assam (India) and washed thoroughly with distilled water to remove dust particles. After the washing process, the fruit was boiled and refluxed in a round bottomed flask with a certain amount of distilled water to extract the juice. The juice was collected and filtered through a Whatmann filter paper no. 41 to remove the small fibers of the fruit.

Synthesis of silver nanoparticles using *Coccinia grandis* fruit extract

Fruit extract (50 mL) and the $AgNO_3$ (0.01M, 50 mL) solution together were added in a container and stirred at room temperature. After 30 min. the green colour of the fruit extract changed to brown colour which indicates the formation of silver nanoparticles (Scheme1).

Catalytic activity of the synthesized silver nanoparticle

In a standard quartz cuvette, having 1 cm path length, 2 mL of water and 60 µL of (6.07×10^{-3} M) nitro compounds (PNP and PNA) were taken separately and the cuvette was then placed in a UV-Vis spectrometer and the absorbance was recorded. To each of these nitro compound solutions, 350 µL of aqueous $NaBH_4$ (0.1 M) was added and the absorbance was noted. Thereafter, 150 µL of 10% Ag NPs solution was added to that mixture and the absorbance was recorded till the peak due to the nitro compounds were completely vanished.

Characterization of silver nanoparticles

Absorption spectra were recorded on Cary 100 BIO UV-Visible spectrophotometer. The prepared Ag NPs were characterized by powder XRD method using Phillips X'Pert PRO diffractometer with CuK radiation of wavelength 1.5418 Å. The morphology and diffraction pattern were determined by JEM-2100 Transmission Electron Microscope. The Infrared spectrum of Ag NPs was recorded by Bruker Hyperion 3000 FTIR spectrometer. The element analysis of the synthesized nanoparticles was performed using EDX on the SEM. The freeze-dried nanoparticles were mounted on specimen stubs with double-sided taps, examined under FEG-SEM, Model: JSM-7600F, Magnification: x25 to 1,000,000a and then the EDX spectrum of spherical NPs was recorded.

Results and Discussion

UV-Visible Analysis

Ag nanoparticles have a unique phenomenon known as surface plasmon resonance (SPR) due to it gives absorption in the UV-Visible region at about 400-450 nm.

X-Ray diffraction (XRD) studies

Figure 1 showed the characteristic XRD peaks of the synthesized Ag nanoparticles. In the Fig. 1 the peaks at 32.8^0, 38.2^0, 44.5^0, 66.4^0, 77.2^0 and 82^0 corresponded to the lattice planes of (101), (111), (200), (220), (311) and (222) reflected the face centered cubic (fcc) structure of Ag (JCPDS file: 65-2871). To calculate the average crystallite particle sizes of the synthesized Ag nanoparticles, the most intense peaks of Ag were preferred. It was calculated

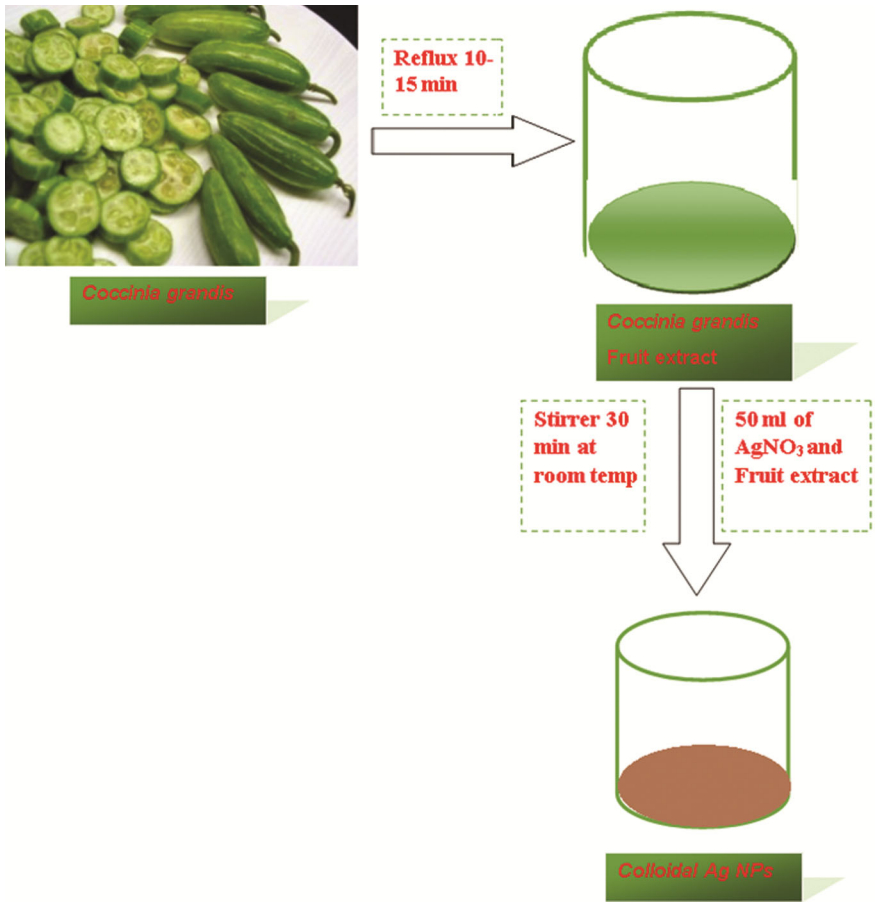

Scheme 1 — Schematic representation of the formation of silver nanoparticle using *Coccinia grandis* fruit extract.

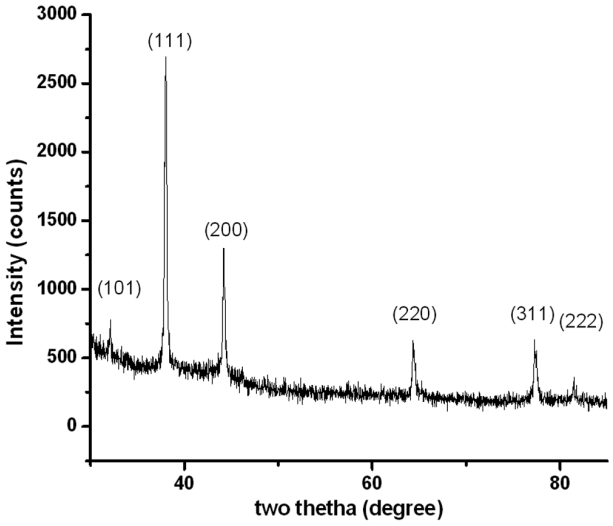

Fig. 1 — XRD spectra of the synthesized Ag nanoparticle.

by Scherrer equation $d = K\lambda/\beta\cos\theta$, where d is the average crystalline particle size; K is a dimensionless shape factor, with a value close to unity (0.9); λ is the X-ray wavelength; β is the line broadening at half the maximum intensity (FWHM); θ is the Bragg angle of the crystal plane.

The highly intense and narrow diffraction peaks revealed the highly crystalline nature of the synthesized nanoparticles. The calculated average crystallite particle size of Ag NPs was found to be 16 nm.

Morphology study

The morphology and size of Ag NPs have been analyzed using TEM studies. Fig. 2 (a-c) corresponds to the TEM, HR-TEM and SAED pattern of the synthesized Ag NPs. The TEM images revealed that the particles are spherical in morphology. The average particles size of the synthesized Ag nanoparticles was found to be 25-30 nm (Fig. 2a). It could also be seen that the NPs are well separated from each other indicating good capping and absence of aggregation. The lattice spacing of the synthesized NPs are calculated from the HR-TEM image (Fig. 2b) and found to be 0.26 nm and corresponds to (111) lattice of face centered cubic (fcc) structure of Ag nanoparticles. The concentric diffraction rings of

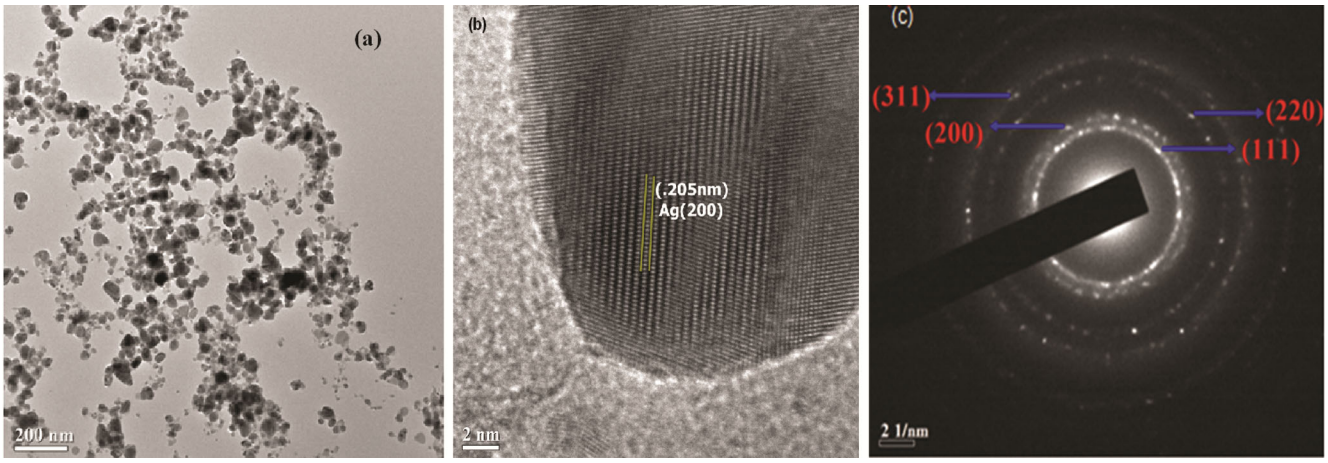

Fig. 2 — (a) TEM, (b) HR-TEM and (c) SAED patterns of the synthesized Ag nanoparticles

SAED pattern (Fig. 2c) showed that the synthesized NPs are polycrystalline in nature and also supports the unit cell structure of Ag nanoparticles.

FT-IR spectroscopy study

Figure 3 (a-b) presents the FT-IR spectra of *Coccinia grandis* fruit extract and synthesized Ag nanoparticles. The FT-IR analysis was carried out to identify functional groups (in the fruit extract) was responsible for the formation of the nanoparticles. The FT-IR studies showed sharp absorption peaks located at 3462, 2082, 1641 and 682 cm^{-1} (fruit extract). The appearance of an intense absorption band around 3462 cm^{-1} corresponds to hydrogen bonded O-H stretching vibrations of alcohols and phenols and also to the presence of amines N-H group in fruit extract. But the peak at 3462 cm^{-1} was shifted to 3410 cm^{-1} in the FT-IR spectra of silver nanoparticles. The shifting of peaks from 3462 to 3410 cm^{-1} (Fig. 3b) may indicate the strong involvement of -OH functional group in the reduction and help in the formation of nanoparticles.

The remaining peaks (fruit extract) at 2082, 1641, 682 cm^{-1} were attributed due to aliphatic C-H stretching in methyl and methylene groups, >C=O stretching and N–H wagging or out of plane O–H bending vibrations respectively.

The peaks (Ag NPs) at 2982, 1641, 1392 and 1062 cm^{-1} indicate the presence of CH stretching groups, -C=O asymmetric stretching vibration and C-N stretching vibration of aromatic and aliphatic amides and presence of amine group, respectively.

Energy dispersive X-ray spectroscopy

EDX is a semi quantitative technique used to identify the elements present in the synthesized Ag NPs. The EDX spectra clearly revealed strong peaks at around 2.8-3 keV which are due to the presence of Ag (Fig. 4).

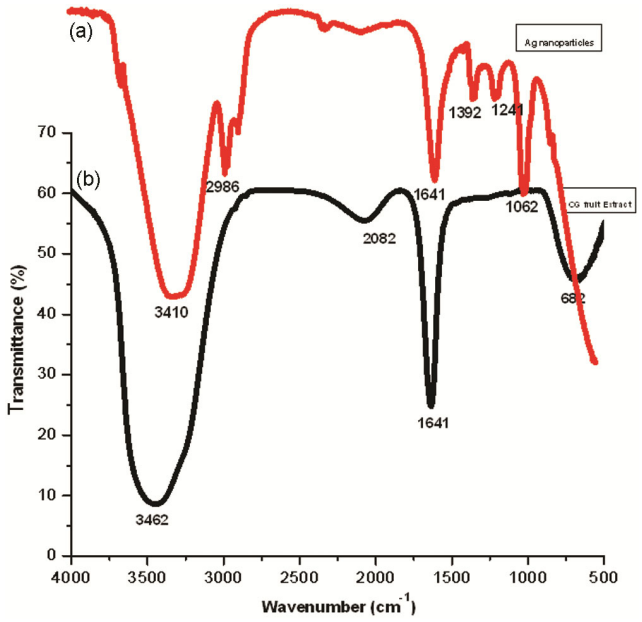

Fig. 3— (a-b) FT-IR spectra of the *Coccinia grandis* fruit extract Ag nanoparticles

Catalytic study for the reduction of PNP and PNA using silver nanoparticles as a calatyst

The catalytic efficiency of synthesized Ag NPs were investigated by carrying out reduction of toxic nitro phenols like *para* nitrophenol and *para* nitroaniline to amino compounds in aqueous medium using $NaBH_4$.

The PNP showed a maximum absorbance at 317 nm in aqueous medium (Fig. 5a). The subsequent addition of freshly prepared $NaBH_4$ solution to PNP leads to a red shift from 317 to 400 nm. It is also observed that

light yellow colour of PNP solution changes to intense yellow due to the formation of *para* nitrophenolate ions under alkaline condition. The peak at 400 nm remain unaltered after a couple of days in absence of any catalyst. This reaction is thermodynamically favorable however, kinetically restricted in the absence of any catalyst due to the large potential difference between PNP and BH_4^-. Therefore, PNP reduction doesn't take place using only the reducing agent $NaBH_4$ in the absence of any catalyst

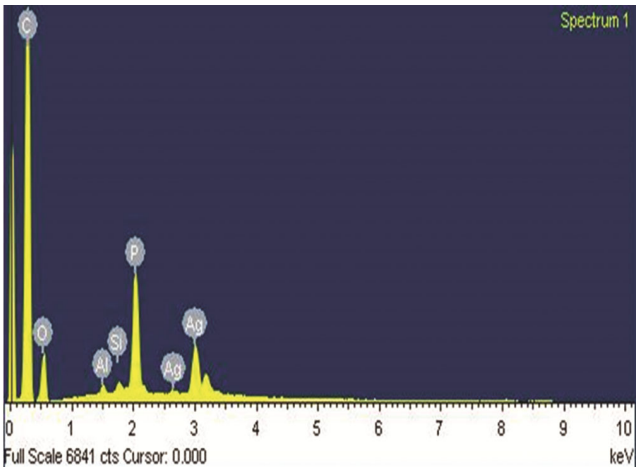

Fig. 4 — EDX spectra of the synthesized Ag nanoparticle

However, after the addition of silver nanoparticles (150 µL of 0.008 g of Ag NPs) the absorption maximum at 400 nm gradually decreases with time which indicate the reduction of PNP and finally disappeared on complete reduction of PNP. This decolorization was monitored by UV-Visible spectroscopy at a regular interval of time. Fig. 5(b) showed the UV-visible spectra for the reduction of PNP. From Fig. 5(b) it is evident that with an increase in time the characteristic peak for PNP decreases with simultaneous appearance of a new peak centered at 300 nm. This is due to the reduction of PNP to PAP. Hence, it is found that PNP can be completely reduced into PAP using Ag nanoparticles as a catalyst in the presence of $NaBH_4$. About 98.3% of PNP was

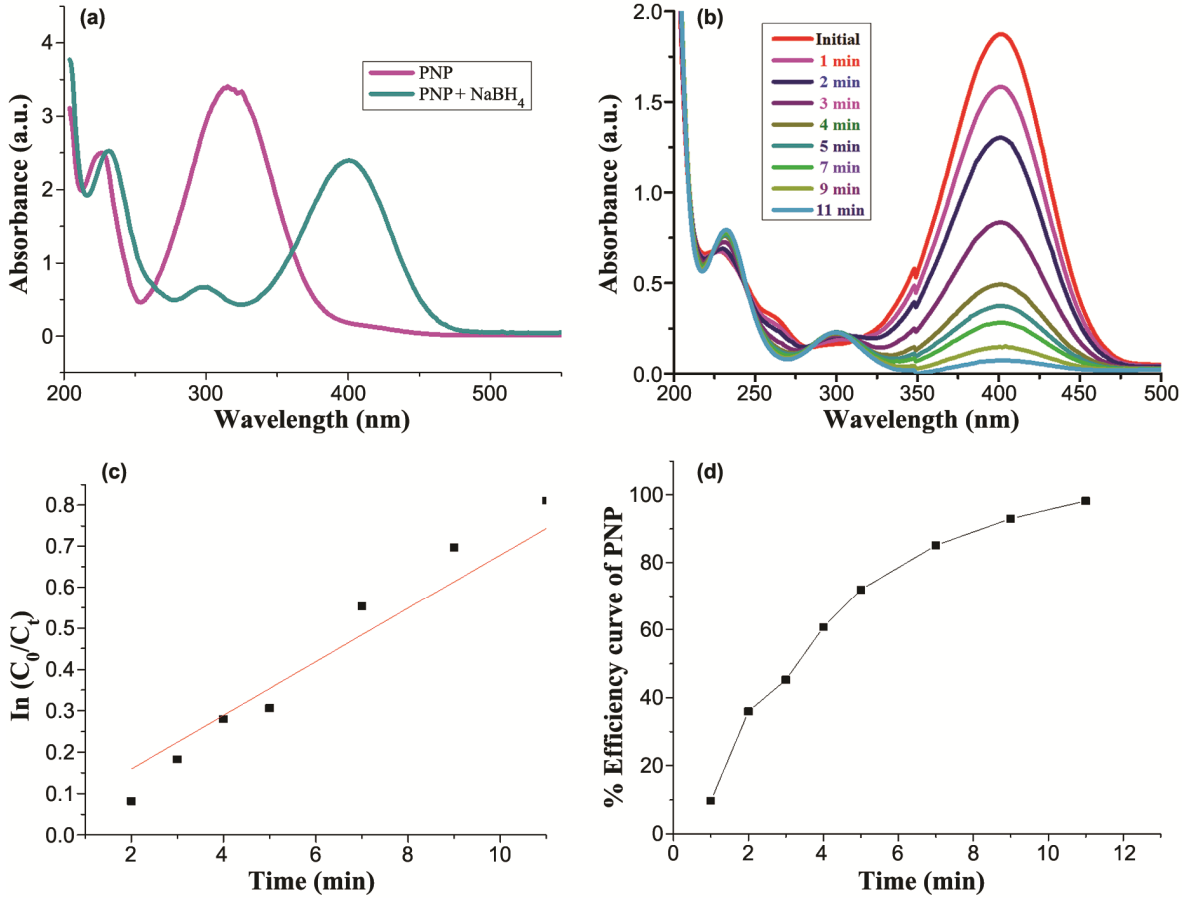

Fig. 5 — (a) Absorption spectra of para nitrophenol and para nitrophenol with $NaBH_4$; (b) Absorption spectra of the reductions of para nitrophenol using Ag NPs as a catalyst in presence of $NaBH_4$; (c) plot of ln[Co/Ct] vs time required reduction and (d) efficiency curve for the reduction of PNP

catalytically reduced within 11 min using Ag nanoparticles. The rate constant (k) has been determined following pseudo first order kinetic from the linear plot of $\ln(C_0/Ct)$ versus time (t) and found to be 4.2×10^{-2} min^{-1} (Fig. 5c). Figure 5d display the efficiency curve for the reduction of *para*-nitrophenol using AgNPs. In this protocol, based on the Langmuir–Hinshel wood model we could discuss the mechanism of reduction of aromatic nitro-compounds to corresponding aromatic amino compounds by $NaBH_4$ in the presence of the Ag nanoparticles as nanocatalysts (Scheme 2). The reduction of nitroaniline, has been also achieved by Ag NPs as a catalyst in presence of $NaBH_4$ as a reducing agent. The peaks at 380 nm due to PNA, after treating with $NaBH_4$ aqueous solution in presence of Ag NPs as a catalyst a new peak generated at 300 nm were for *para* phenylenediamine. The formation of new peaks at 300 nm was due to the reduced product *para* phenylenediamine. It was also observed that with increase in time the characteristic peak for PNA decreases with simultaneous appearance of a new peak centered at 300 nm. Fig. 6 (a) represents the absorption spectra of the reduction of *para* nitroanilne using silver nanoparticles. Approximately, 98% reduction of PNA was reduced within 11`min using Ag nanoparticles. The reduction also followed the pseudo first order kinetics (Fig. 6b) and rate constant was found to be 5.3×10^{-2} min^{-1} respectively.

Mechanism of reduction of para nitrophenol and para nitroaniline by Ag nanoparticles in presence of $NaBH_4$

The catalytic action of biogenic Ag NPs in the reduction of *para* nitrophenol and *para* nitroaniline by use of $NaBH_4$ can be explained in terms of Langmuir–Hinshelwood model (Scheme 2). The mechanistic pathway for the hydrogenation of *para* nitrophenol involves the following steps: (i) transfer of electrons to the nitro compounds (PNP and PNA) and (ii) proton availability. In this model, $NaBH_4$ acts as electron donor and as a hydrogen supplier. For the reduction of *para* nitrophenol and *para* nitroaniline, electron is required to be transferred from the donor BH_4^- ion. In presence nanoparticles (Ag), BH_4^- ion gets adsorbed on its surface and the discharge of electrons from BH_4^- ion takes place through the metal to the acceptor i.e., *para* nitrophenol and *para* nitroaniline[23-25]. The aqueous medium, which is a polar protic solvent, provides the required amount of H^+ ion for the complete reduction of *para* nitrophenol and *para* nitroaniline.

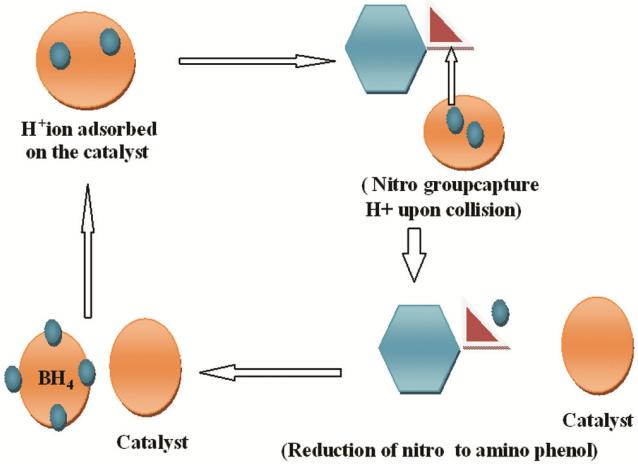

Scheme 2 — Mechanism for the reduction of zpnzp to PAP using of Ag NPs as a catalyst in presence of $NaBH_4$ in aqueous medium

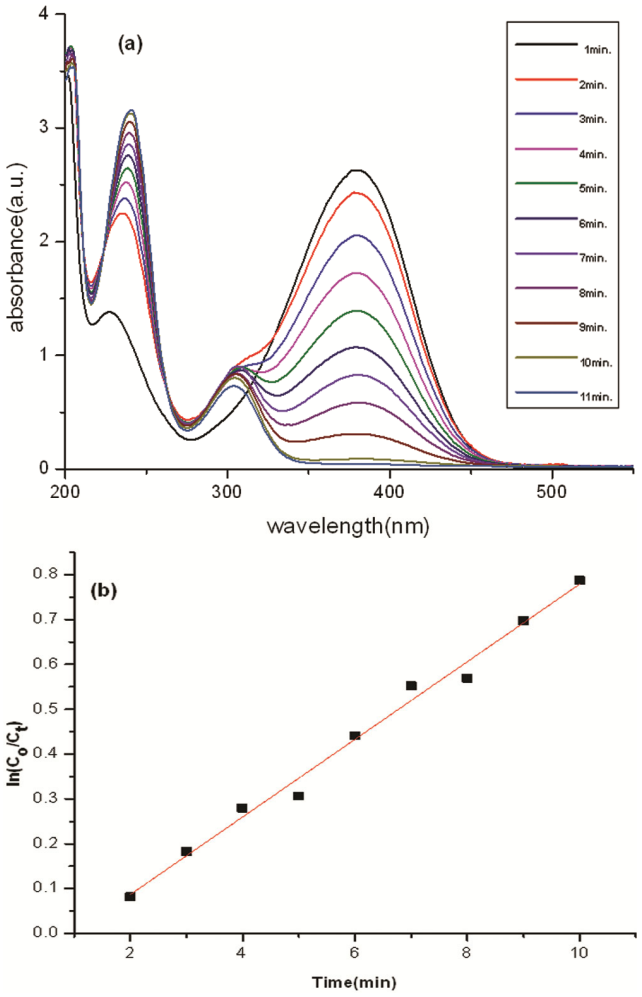

Fig. 6 — (a) Absorption spectra of the reductions of para nitroaniline using Ag as a catalyst in presence of $NaBH_4$ and (b) plot of ln[Co/Ct] vs time required reduction.

Conclusion

In a nutshell, it is evident that a green method may be developed for the synthesis of Ag nanoparticles using *Coccinia grandis* fruit extract. The present method is simple, green, environment friendly and free of the use of any organic solvents. The phyto-chemical present in the fruit acts as reducing as well as stabilizing agent in the synthesis of Ag nanoparticles. The TEM image suggests that the synthesized nanoparticles are spherical in nature and well separated. The UV-Visible spectroscopy, HR-TEM, SAED pattern, XRD, and EDX spectroscopic analyses confirm the formation of Ag nanoparticles. The synthesized plasmonic catalyst Ag nanoparticles are successfully utilized for the reduction of *para* nitrophenol and *para* nitroaniline. From the reduction, it is also observed that the Ag NPs show excellent catalytic activities towards the removal (reduction process) of toxic nitro compounds.

Acknowledgement

The authors are grateful to SAIF–NEHU Shillong, CSMCRI Gujarat and SAIF- IIT Bombay for providing the TEM, XRD, FT-IR and EDX facilities, respectively.

References

1 Sivanesan A, Ly H K, Kozuch J, Sezer M, Kuhlmann U, Fischer A & Weidinger I M, *Chem Commun*, 47 (2011) 3553.
2 Liu K, Qu S, Zhang X, Tan F & Wang Z, *Nanoscale Res Lett*, 8 (2013) 1.
3 Zhu H, Du M, Zhang M & Yao J, *Biosens Bioelectron*, 49 (2013) 210.
4 Zhang P, Shao C, Zhang Z, Zhang M, Mu J, Guo Z & Liu Y, *Nanoscale*, 3 (2011) 3357.
5 Devi T B & Ahmaruzzaman M, *Chem Eng J*, 317 (2017) 726.
6 Husseiny M I, El-Aziz M A, Badr Y & Mahmoud M A, *Spectrochim Acta Part A*, 67 (2006) 1003.
7 Sastry M, Ahmad A, Khan M I & Kumar R, *Curr Sci*, 85 (2003) 162.
8 Nakkala J R, Mata R, Gupta A K & Sadras S R, *Eur J Med Chem*, 85 (2014) 784.
9 Sun Q, Cai X, Li J, Zheng M, Chen Z & Yu C P, *Colloid Surf A,* 444 (2014) 226.
10 Nabikhan A, Kandasamy K, Raj A & Alikunhi N M, *Colloids Surf B ,* 79 (2010) 488.
11 Mariselvam R, Ranjitsingh A J, Usha Raja Nanthini A, Kalirajan K, Padmalatha C & Mosae Selvakumar P, *Spectrochim Acta Part A*, 129 (2014) 537.
12 Sadeghi B, Rostami A & Momeni S S, *Spectrochim Acta Part A,* 134 (2015) 326.
13 Sadeghi B & Gholamhoseinpoor F, *Spectrochim Acta Part A,* 134 (2015) 310.
14 Santhoshkumar T, Rahuman A A, Rajakumar G, Marimuthu S, Bagavan A & Jayaseelan C, *Parasitol Res*, 108 (2011) 693.
15 Krishnaraj C, Jagan E, Rajasekar S, Selvakumar P, Kalaichelvan P & Mohan N, *Colloids Surf B,* 76 (2010) 50.
16 Kumar S, Daimary R M, Swargiary M, Brahma A, Kumar S & Singh M, *Int J Pharm Biol Sci,* 4 (2013) 378.
17 Vijay Kumar P P N, Pammi S V N, Kollu P, Satyanarayana K V V & Shameem U, *Ind Crops Prod*, 52 (2014) 562.
18 Gopinath V, Mubarak Ali D, Priyadarshini S, Priyadharsshini N M, Thajuddin N & Velusamy P, *Colloids Surf B,* 96 (2012) 69.
19 Ashokkumar S, Ravi S, Kathiravan V & Velmurugan S, *Spectrochim Acta A*, 134 (2015) 34.
20 Arunachalam R, Dhanasingh S, Kalimuthu B, Uthirappan M, Rose C & Mandal A B, *Colloids and Surf B*, 94 (2012) 226.
21 Visvanathan S, Janathul F S & Bharathi V, *WJPPS*, 3 (2014) 1777.
22 Ruby S, Banurekha J, Loganathan J & Jaykar B, *AJPAMC,* 2 (2014) 183.
23 Immanuel Edison T N J, Sethuraman M G S & Lee Y R, *Res Chem Intermed*, 42 (2016) 713.
24 Lunhong A & Jing J, *Bioresour Technol*, 132 (2013) 374.
25 Aditya T, Pal A & Pal T, *Chem Commun*, 51 (2015) 941.